Experimental validation of a full Stokes spectropolarimeter for space applications

Mr. Vasilescu, B.V.; Piron, P.; Veenstra, Allard; Snel, Ralph ; Di Iorio, Eugenio Iorio; Ouellet, Mireille ; Chavet, Quentin ; Ferrario, Ivan; Loicq, J.J.D.

DOI
10.1117/12.3018645

Publication date
2024

Document Version
Final published version

Published in
Space Telescopes and Instrumentation 2024: Optical, Infrared, and Millimeter Wave

Experimental validation of a full Stokes spectropolarimeter for space applications

Bogdan Vasilescu[a], Pierre Piron[a], Fabien Schmutz[a], Ralph Snel[b], Eugenio Di Iorio[b], Mireille Ouellet[b], Quentin Chavet[b], Ivan Ferrario[b], and Jérôme Loicq[a,c]

[a]Technische Universiteit Delft, Kluyverweg 1, 2629 HS Delft, Netherlands
[b]TNO, Stieltjesweg 1, 2628 CK Delft, Netherlands
[c]Université de Liège - STAR Institute, Allée du Six Août 19C, B-4000 Liège, Belgium

ABSTRACT

During the last few years, one of our main research topics has been developing a new type of spectropolarimeter intended for space applications. Initially analyzed numerically, the instrument has a compact, stable design without rotating components. The entire Stokes vector can be determined in a single shot in a vast spectral range. The simulations proved that the modulation schemes that can be obtained for this instrument are close to the optimal form. The objective of the current research is the experimental validation of this instrument. Here, we present the first results for determining the instrumental matrix and the demodulation results for a series of polarization states. In conclusion, we present the possible further developments of that project.

Keywords: Polarimetry, Spectropolarimetry, Optics, Space instrumenetation

1. INTRODUCTION

The state of polarization of light is a formidable scientific tool that has gained remarkable notoriety in recent years. The interest in determining this property of light is manifested in the most diverse fields. Today, we use polarization on a large scale in astronomy,[1] space awareness,[2] climate studies,[3] biology, chemistry, medicine,[4] defense,[5] etc. Despite the growing interest of the scientific community in determining this property of light, the space field still lacks high-performance instruments capable of determining any polarization. The reason is represented by the limitations of the current spectropolarimeters and the risks they can bring to space missions. Most instruments intended for the space environment offer access to a narrow range of polarization states or are characterized by a large volume, rotating elements, and a limited field of view.

In this context, we started the research of a new instrument capable of determining with high precision any polarization that would satisfy the most intransigent demands of a space mission. Our previous publications[6,7] presented a possible candidate for such an instrument. It is an innovative concept for the snapshot determination of polarization in a vast spectral range. Although it uses the amplitude division technique, it has the advantage of a minimal volume and a compact and static structure.[8]

We have demonstrated in previous research that such an instrument is characterized by uniqueness,[6] meaning that each polarization state corresponds to a single intensity pattern in the detector plane and only one. Moreover, the modulation schemes that can be obtained converge towards an optimal form,[7] thus guaranteeing an equal impact of the noise on determining the Stokes parameters.

The current paper presents the first steps towards the experimental validation of the concept. Here, we present the determination of the instrumental matrix and the results of a first demodulation test at a wavelength of 514.5 nm, performed on 180 elliptical polarization states. The results demonstrate the ability of the new instrument to determine all these polarization states in a single shot.

We conclude this communication with the lessons learned throughout the experimental activities and discuss future research directions.

Further author information: (Send correspondence to Pierre Piron)
Pierre Piron.: E-mail: P.Piron@tudelft.nl

Space Telescopes and Instrumentation 2024: Optical, Infrared, and Millimeter Wave, edited by Laura E. Coyle, Shuji Matsuura, Marshall D. Perrin, Proc. of SPIE Vol. 13092, 130922W · © 2024 SPIE · 0277-786X · doi: 10.1117/12.3018645

2. THE CONCEPT OF THE INSTRUMENT

As with all spectropolarimeters, the instrument shown here comprises a modulator, a linear polarimeter (analyzer), and a dispersive element or filter. The essential part, which has been the subject of our previous research, is the modulator. Built from a birefringent material (MgF_2 in the present case), this modulator has a triple prismatic structure, as can be seen in Fig.1. The geometry and positioning of the fast axes were chosen so that the maximum effectiveness of the modulation scheme could be obtained for the entire Stokes vector and to minimize the beam-splitting effect and internal reflections. The first prism on the left side has an apex angle of 2.6°, a height of 2 cm, and a width of 2 cm, and its fast axis is parallel to the Ox axis. In addition, the thickness at the tip is 1 mm to ensure the solidity of the component. The third prism has an apex angle of 1.8° and the same width and height as the first prism. Also, the thickness at the tip is 1 mm. However, its fast axis is oriented at 45° with respect to Ox in the xy plane. The intermediate prism plays a binding role. Its dimensions ensure that the input and output faces of the modulator are parallel. For this, a thickness at the tip of 1 mm was foreseen. However, its fast axis is oriented along the Oz axis, which is also the direction of light propagation. For this reason, it has no impact on the light phase.

The working principle of a spectropolarimeter employing the above modulator is illustrated in Fig.1. The light arriving collimated from the left side passes through the modulator and a linear polarizer before arriving on the detector (CCD). A filter or a dispersive element should be introduced to select a particular wavelength between the linear polarizer and the CCD. The light arriving on the modulator, which can be partially or entirely polarized, will be modulated in intensity in the Oy direction. However, the unpolarized light will not be modulated since it passes unaffected through the modulator. Each polarization state will generate a particular intensity pattern in the detector plane along the vertical. This pattern is related to the wavelength and the type of polarization. The ideal expression of the intensity detected by a pixel situated at the level y, at the wavelength λ, when the light carrying the state of polarization $S = (S_0, S_1, S_2, S_3)^T$ passes through the system is:

$$I(y,\lambda,\theta) = \frac{1}{2}\left(S_0 + S_1 \cdot m(y,\lambda,\theta) + S_2 \cdot n(y,\lambda,\theta) + S_3 \cdot p(y,\lambda,\theta)\right), \tag{1}$$

where the modulation functions m, n and p are:

$$\begin{cases} m(y,\lambda,\theta) = \cos(2\theta)\cos(\phi_3) \\ n(y,\lambda,\theta) = \sin(2\theta)\cos(\phi_1) + \cos(2\theta)\sin(\phi_1)\sin(\phi_3) \\ p(y,\lambda,\theta) = \sin(2\theta)\sin(\phi_1) - \cos(2\theta)\cos(\phi_1)\sin(\phi_3) \end{cases}, \tag{2}$$

and the phases corresponding to the first (ϕ_1), respectively, the third prism (ϕ_3) are:

$$\begin{cases} \phi_1 = \frac{2\pi}{\lambda}\Delta n(\lambda)(d_0 + (h-y)\tan(\xi)) \\ \phi_3 = \frac{2\pi}{\lambda}\Delta n(\lambda)(d_0 + (h-y)\tan(\psi)) \end{cases}, \tag{3}$$

where ϕ_1 is the phase determined by the first prism from the left (see Fig.1), of apex angle ξ and ϕ_3 is the phase induced by the third prism, of apex angle ψ. The orientation of the analyzer with respect to the Ox axis is given by the angle θ. $\Delta n(\lambda)$ represents the birefringence of the medium, d_0 the thickness of the wedges at the top, and h the height of the modulator.

The polarized light that passes through the modulator is thus modulated in intensity by the functions m, n and p presented in Eq.(2). For a column of N pixels in the detector plane, the intensity values detected by each pixel can be expressed as:

$$\begin{pmatrix} I_1 \\ I_2 \\ I_2 \\ . \\ . \\ I_N \end{pmatrix} = \underbrace{\frac{1}{2}\begin{pmatrix} 1 & m(y_1) & n(y_1) & p(y_1) \\ 1 & m(y_2) & n(y_2) & p(y_2) \\ 1 & m(y_3) & n(y_3) & p(y_3) \\ . & . & . & . \\ . & . & . & . \\ 1 & m(y_N) & n(y_N) & p(y_N) \end{pmatrix}}_{W} \cdot \begin{pmatrix} S_0 \\ S_1 \\ S_2 \\ S_3 \end{pmatrix}, \tag{4}$$

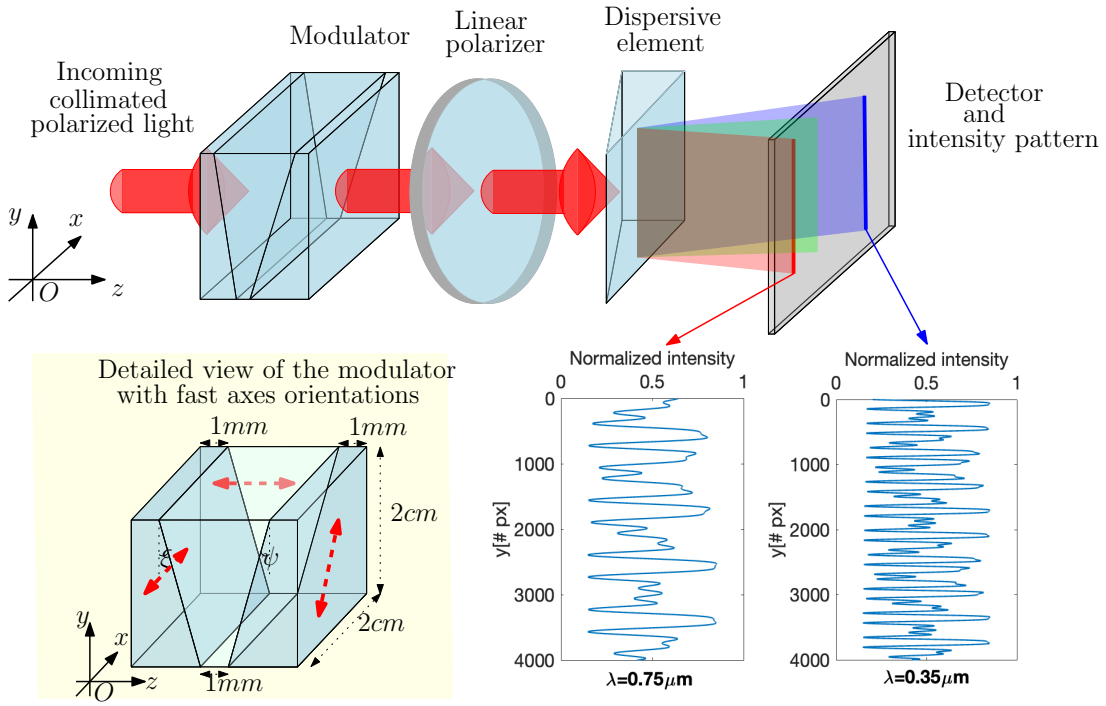

Figure 1. Schematic representation of the working principle of the spectropolarimeter. The light, arriving collimated from the left side, passes through a modulator, a linear polarizer, and, eventually, through a dispersive element or a filter. A specific intensity pattern in the detector plane will characterize any polarization state. The critical component, the modulator, has a triple prismatic structure, with the fast axes differently oriented.

or, in a vectorial form:

$$\vec{I} = W \cdot \vec{S}. \tag{5}$$

Thus, any incoming polarization can be retrieved via

$$\vec{S} = W^{-1} \cdot \vec{I}. \tag{6}$$

The difficulty with this expression is that, in practice, the modulation matrix W differs from its theoretical expression. The misalignment of the three prisms, the imprecision of the analyzer's orientation, or lack of homogeneity determine such a difference. This research aims to determine the instrumental matrix (W^{-1}) and test the demodulation process on different types of incident polarizations.

3. METHOD

The immediate solution to the problem related to the determination of the instrumental matrix would be to calculate, for an already known vector $\vec{S}$:

$$W^{-1} = S \cdot \vec{I}^{-1}, \tag{7}$$

and to use for the inversion of the vector $\vec{I}(N \times 1)$ the pseudo-inverse formula:

$$I^{-1} = I^T \cdot (I \cdot I^T)^{-1}. \tag{8}$$

Unfortunately, the $I \cdot I^T$ product is ill-conditioned,[9] and the product $I \cdot I^T$ cannot be inverted. Therefore, the pseudo-inverse of I cannot be used here. Another approach should be used to solve the problem. This is based on the findings of Boulbry,[9] extending the principle of the method from an instrument in which the modulation

is produced by varying the orientation of the analyzer to our instrument, where the modulation results from the phase variation inside the modulator.

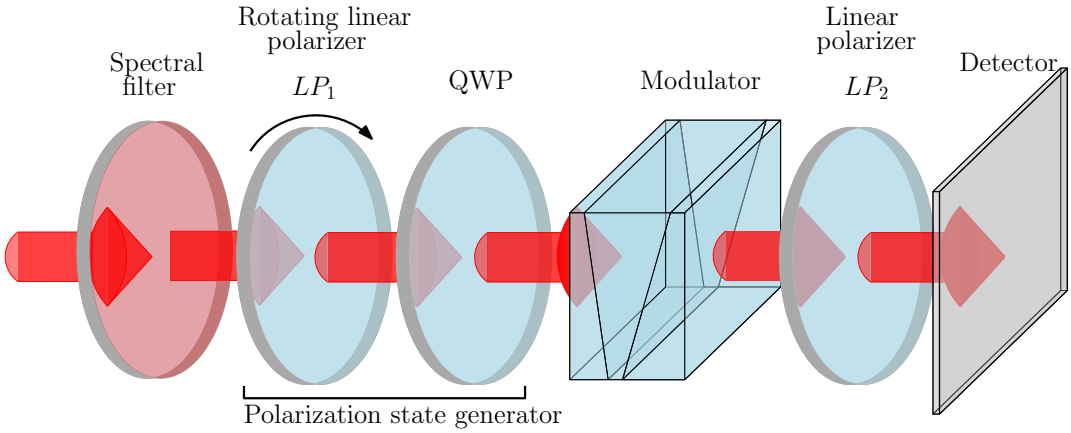

Figure 2. Representation of the optical setup used to determine the instrumental matrix. The collimated light from the left side passes through a spectral filter, then a polarization state generator (PSG), through the modulator and a linear polarizer.

Therefore, by measuring successively M incoming states of polarisation (well-known), chosen from the Poincaré sphere, then, for a column of N pixels, the Eq.(4) becomes:

$$\begin{pmatrix} I_1^1 & I_1^2 & . & . & I_1^M \\ I_2^1 & I_3^2 & . & . & I_3^M \\ I_3^1 & I_3^2 & . & . & I_3^M \\ . & & & & \\ . & & & & \\ I_N^1 & I_N^2 & . & . & I_N^M \end{pmatrix} = W \cdot \begin{pmatrix} S_0^1 & S_0^2 & . & . & S_0^M \\ S_1^1 & S_1^2 & . & . & S_1^M \\ S_2^1 & S_2^2 & . & . & S_2^M \\ S_3^1 & S_3^2 & . & . & S_3^M \end{pmatrix}. \tag{9}$$

The supra-script $(1:M)$ designates the test or the polarization state used as input. In a contracted form, this relation can be expressed as,

$$[\vec{I}] = W \cdot [\vec{S}], \tag{10}$$

$[\vec{I}]$ being an $N \times M$ matrix, and $[\vec{S}]$ a $4 \times M$ matrix. In this new context, the relation (7) becomes:

$$W^{-1} = [\vec{S}] \cdot [\vec{I}]^{-1}. \tag{11}$$

Because $[\vec{I}]$ is an $N \times M$ matrix, it can be decomposed using the singular value decomposition:

$$[I] = U \cdot D \cdot V^T. \tag{12}$$

In this formulation, U is built with the nonzero eigenvalues (σ_i) of $[I]$. The columns of U are given by:

$$u_i = \frac{1}{\sigma_i}[I]v_i, \tag{13}$$

where v_i is the eignevector corresponding to σ_i. V is the matrix of the eigenvectors of $[I]$, and

$$D = diag(\sigma_1, \sigma_2, \sigma_3, .., 0, 0...., 0). \tag{14}$$

When $\sigma_i = 0$, then the corresponding diagonal term should be replaced by 0. Thus, the inverse of $[I]$ should be written as:

$$[I]^{-1} = V \cdot diag(\frac{1}{\sigma_1}, \frac{1}{\sigma_2}, \frac{1}{\sigma_3}, ..., 0, 0, ..., 0) \cdot U^T. \tag{15}$$

Substituting this value in the relation (11), the instrumental matrix W^{-1} can be obtained.

4. EXPERIMENTAL PROCEDURE

The optical setup used to determine the instrumental matrix is shown in Fig.2. The light produced by a laser-driven source (LDLS) of white light arrives from the left side, passing at first through a collimator and a narrow bandpass spectral filter with 514.5 nm central wavelength, and $FWHM$ =3 nm. Then, the collimated light passes through a rotating linear polarizer (LP_1) and a QWP (Thorlabs, AQWP10M-580). The QWP is followed by the modulator and the second linear polarizer (LP_2), playing the role of the analyzer. After LP_2, the light is collected by a CCD detector (BSF-U3-123S6M) with a pixel size of 3.45 µm.

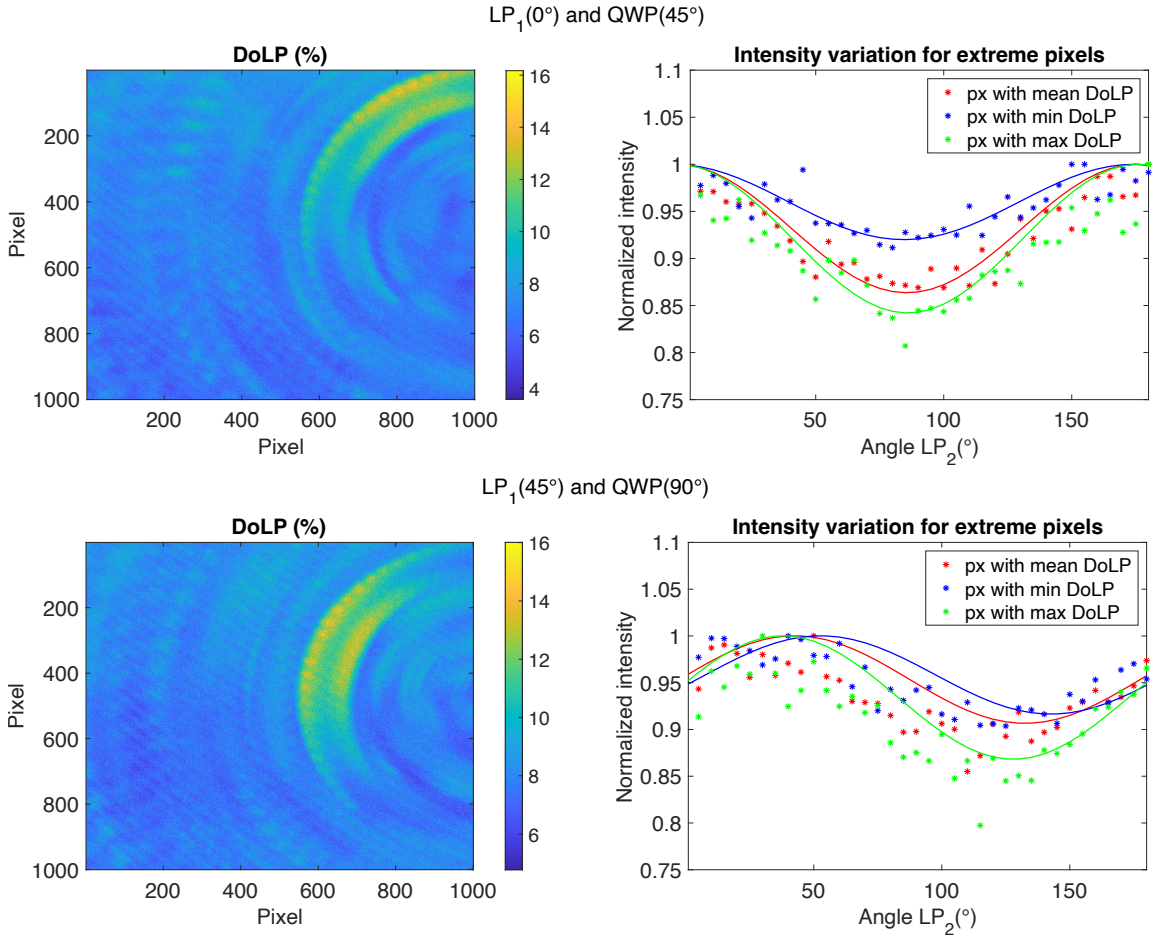

Figure 3. Degree of linear polarization ($DoLP$) obtained with configuarations of the PSG that should produce, theoretically, circular polarization. Ideally, the two configurations should be equivalent. In practice, we notice a slight difference between the two. This is due to a possible misalignement of the QWP. The right-side plots present the intensity variation obtained while turning LP_2 for the pixels that exhibit the maximum, average, and minimum $DoLP$. The continuous lines correspond to the theoretical model adjusted for the best fit.

This optical compound formed by LP_1 and QWP plays the role of a polarization state generator. It allows us to obtain all the necessary states of polarization used as input to retrieve the instrumental matrix. Thus, by

positioning the quarter waveplate with the fast axis horizontal, 180 Stokes vectors were generated by rotating LP_1 with a step of 1°. Then, the procedure was repeated for the wave plate oriented at 90°.

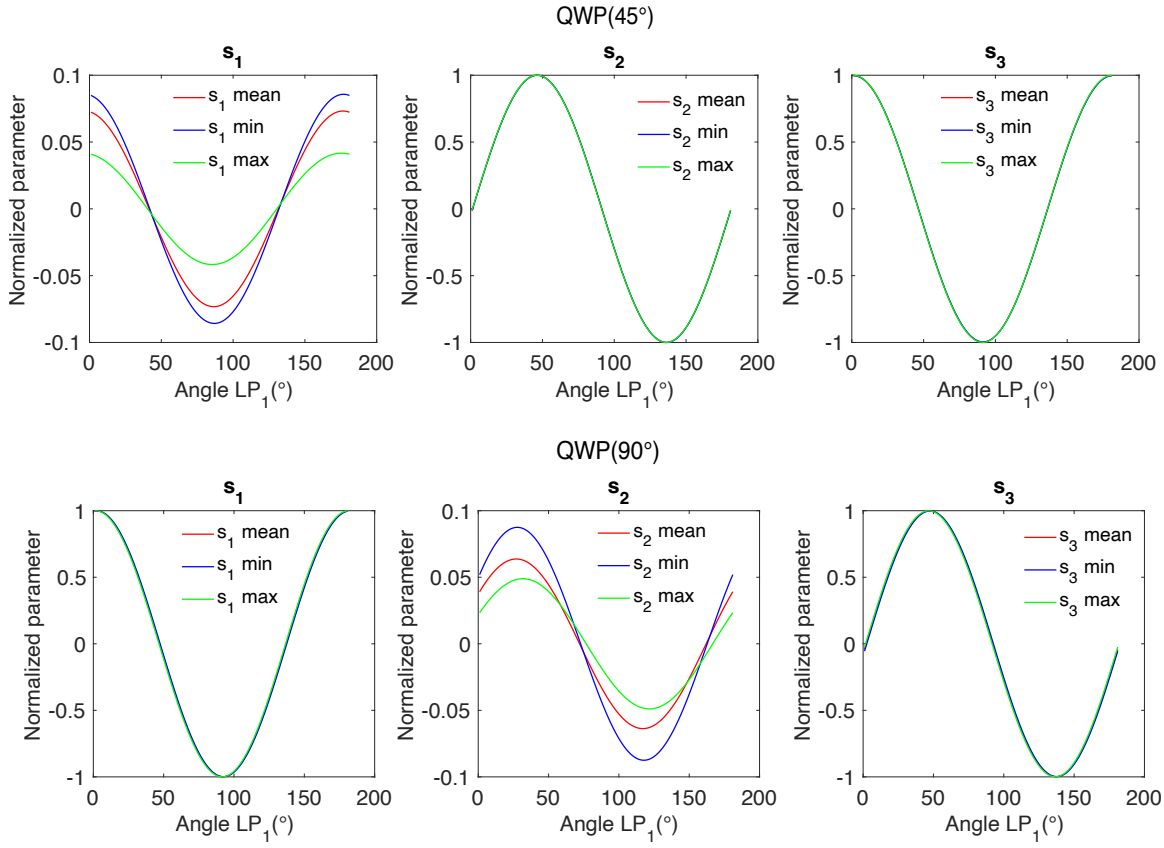

Figure 4. Possible values of the incoming Stokes vectors as inferred from the variation of the $DoLP$ across a single line of pixels.

The precision of determining the instrumental matrix is directly affected by the precision of generating the polarization states. The intensity values are directly read from the images, but the corresponding Stokes vectors must be inferred from the properties and configuration of the polarization generator.

The following strategy was adopted to estimate the used Stokes vectors: after orientating the linear polarizer (LP_1) at 0° and the QWP at 45°, an analyzer (LP_2) placed after the QWP was rotated from 0° to 180°, and images were recorded for each position. In an ideal configuration, the detected light intensity should not vary with analyzer rotation because the polarization generator produces a circular polarization in this configuration. However, according to the datasheet, the QWP does not behave exactly like a QWP at 514.5 nm, and, as a result, a perfect circular polarization cannot be achieved. The maximum is located around 95%. As a result, a residual linear polarization of at least 5% always occurs. The measurements performed for this configuration showed a linear residue between 5% and 15% (see Fig.3). Almost the same values were obtained for the linear polarizer configuration at 45° and QWP at 90°. It is worth noting, however, that the linear polarization mainly affects a particular region in the image, which suggests the effect of a misalignment (see Fig.3).

Then, limiting the analysis to a single vertical line of pixels, we looked for corrections for the orientation of the fast axis of the QWP and for the retardance capable of producing results similar to the experimental ones. We thus looked at the maximum, minimum, and average $DoLP$ values recorded on a line of pixels. This procedure allowed us to estimate the interval in which the fast axis of the QWP is located and the retardance capable of producing the results from the tracked pixel line. Based on this estimate of the QWP, an estimate of the input Stokes vectors can be obtained.

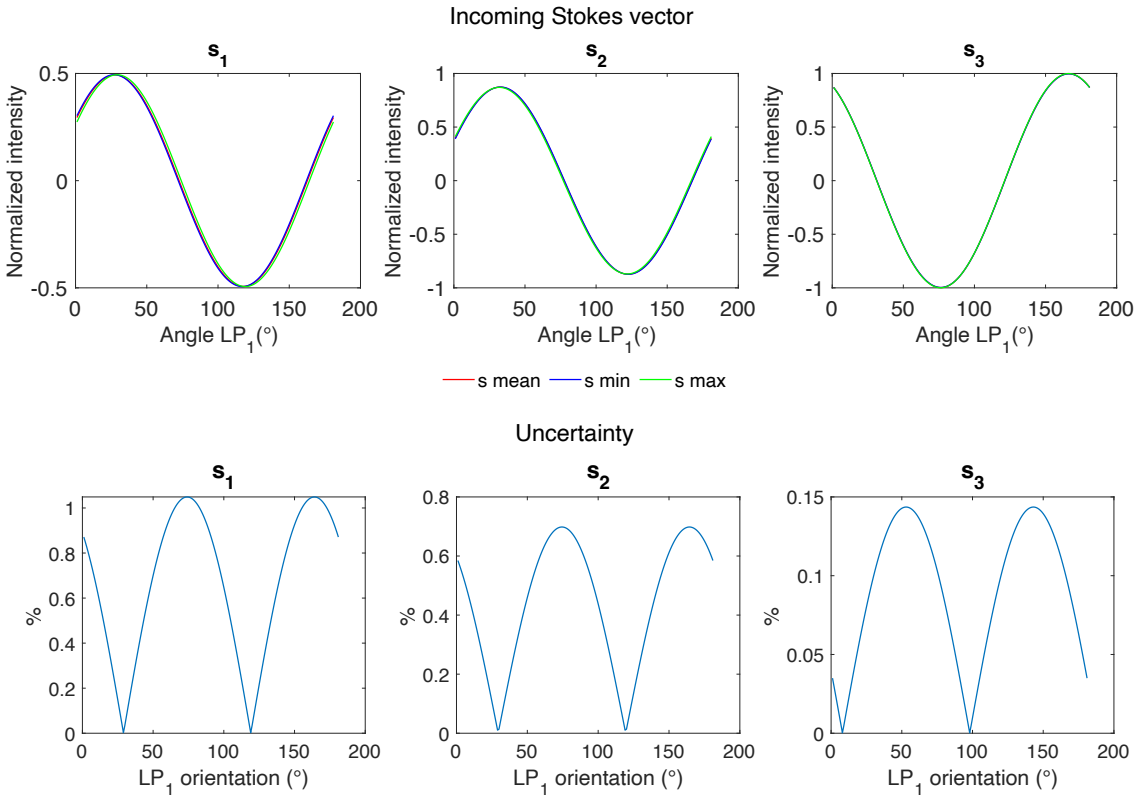

Figure 5. Incoming Stokes parameters corresponding to the states obtained through the rotation of LP_1 for a QWP oriented at 30°. The uncertainty corresponds to the interval of variation of each parameter for every orientation of LP_1.

Therefore, this procedure allows the variation of the $DoLP$ values along a pixel line to be translated by a variation of the Stokes vector generated by the PSG along the same line of pixels. Figure 4 shows the possible values that the generated Stokes vector can embrace starting from this variation of $DoLP$.

The fact that the incoming Stokes vector varies in a specific interval for the given line of pixels also suggests that the instrumental matrix that can be retrieved starting from this input has an interval of uncertainty. Designating with $[S]_{min}$, $[S]_{mean}$, and $[S]_{max}$ the Stokes vectors obtained from the minimal, average, and maximal values of the parameters presented in Fig.4, we can also compute the corresponding values of the instrumental matrix:

$$\begin{cases} W_{mean}^{-1} = [S]_{mean} \cdot [I]^{-1} \\ W_{min}^{-1} = [S]_{min} \cdot [I]^{-1} \\ W_{max}^{-1} = [S]_{max} \cdot [I]^{-1} \end{cases} . \tag{16}$$

These instrumental matrices will give us a range of variations for determining a polarization state.

5. RESULTS

Concerning the demodulation error, assessing it precisely in the given system configuration is impossible. For instance, we can consider the polarization states generated as a test with a rotating LP_1 and QWP oriented at 30°. Like in the previous configurations, each polarization state produced with LP_1 and $QWP(30°)$ will generate an inhomogeneous image on the detector. However, this time, we do not have reference polarization states (as was the case of the circular states before) to track the deviation from the expected intensities. We can only suppose that we stay within the same limits as in the previous cases as long as the system is not altered.

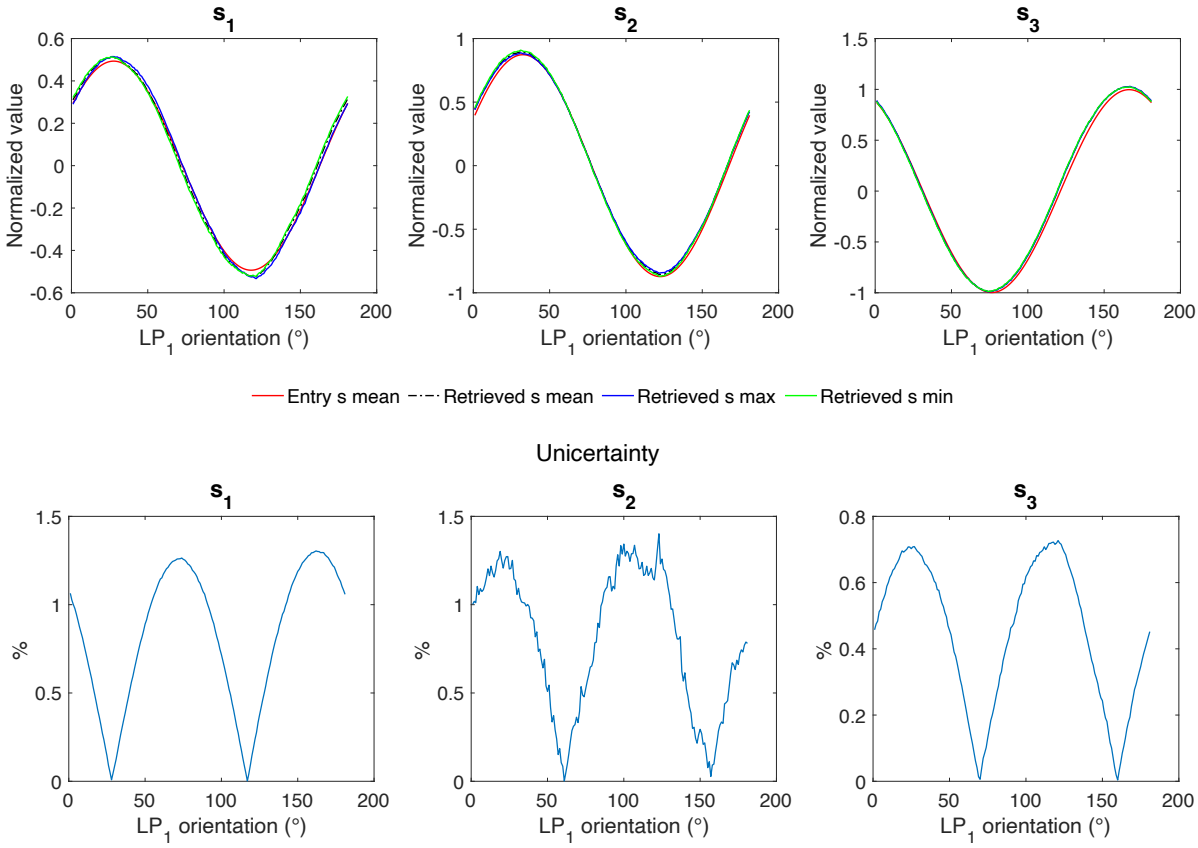

Figure 6. Demodulation of 180 states of polarization obtained by rotating LP_1 in front of the QWP oriented at 30°. The mean value of incoming Stokes parameters is displayed in red, whereas the minimum, mean and maximum values of the retrieved parameters are displayed in green, black and blue.

Therefore, we may say again that the incoming polarization varies across the line of pixels between the limits imposed by the variation of the retardance and the fast axis. Based on these hypotheses, we can build the possible outcome of a rotating LP1 and a QWP oriented at 30°. The results are presented in Fig.5.

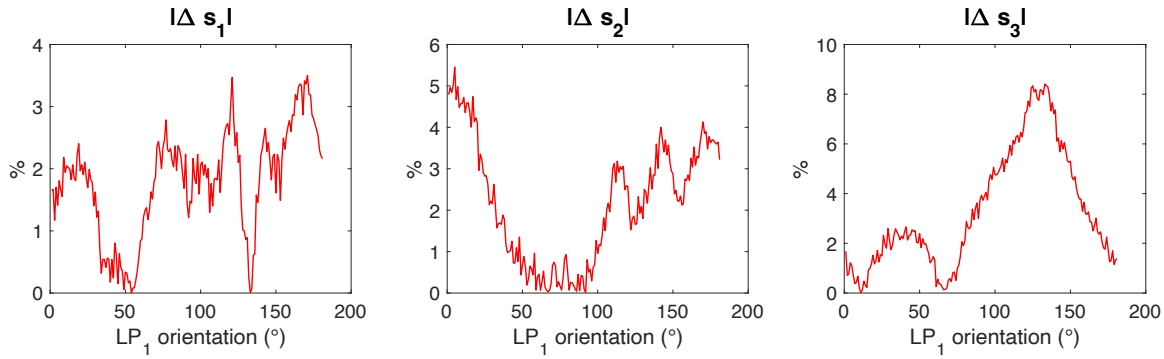

Figure 7. Relative difference between the incoming and demodulated Stokes parameters.

Nevertheless, because we do not dispose of a thorough characterization of the QWP and of the linear polarizers, we cannot tell with enough precision what is the real interval of variation across the line of pixels. Because of this, after demodulation, there is no reference after which to establish an error. To overcome this situation,

a calibrated PSG generator must be used in the beginning to retrieve the instrumental matrix, and then the demodulation should be applied to well-known sources of polarization.

Despite the lack of precision in the PSG functioning and in the misalignment assessment, which cannot be compensated through the adjustment of the QWP properties, the first tests for the demodulation are very promising. In this test, we have tried to retrieve the 180 states of polarization generated by rotating LP_1 in front of a QWP oriented at 30°, states that are presented in Fig.5. The results of the demodulation process are presented in Fig.6. Looking at the interval of variation for each retrieved parameter, we see that the uncertainty is below 1.5% and it corresponds in fact to the variation of the incoming Stokes itself.

Considering the difference between the mean value of the retrieved parameters and the average incoming parameters, we obtain the results from the Fig.7.

A prior characterization of the PSG, comprising a thorough investigation of the optical components, can help reduce the uncertainty on the instrumental matrix and, thus, the errors of the instrument. Still, this can be considered a success for the first attempt at demodulation.

6. CONCLUSION

We demonstrated through this research that a polarimeter based on a triple prismatic architecture, such as the one shown in Fig.1, can be a formidable tool for determining the entire Stokes vector in a single shot. For this purpose, we used a method based on the empirical determination of the instrumental matrix, and the measurements and tests were performed at a single wavelength, λ =514.5 nm. We learned from this approach that a calibrated polarization state generator is vital for a realistic estimate of the instrument's precision.

This would also allow for correcting the modulation functions and thus replace the demodulation process based on the inversion of the W matrix with a simple fit with Eq.(1).

Besides using a pre-calibrated PSG, the next step in investigating this new instrument concept is testing it at other wavelengths and for different bandwidths. Moreover, since the idea is compatible with imaging working mode, its adaptation to facilitate the simultaneous collection of spatial, spectral, and polarimetric data is foreseen.

REFERENCES

[1] Leroy, J.-L., [*Polarization of light and astronomical observation*], CRC Press (2000).

[2] Snel, R. C., Vasilescu, B., Di Iorio, E., Piron, P., Loicq, J., Ferrario, I., and Silvestri, F., "Spectropolarimetry for space object identification," in [*Electro-Optical and Infrared Systems: Technology and Applications XX*], Hickman, D. L., Bürsing, H., Steinvall, O., and Kamerman, G. W., eds., 36, SPIE (2023).

[3] Gassó, S. and Knobelspiesse, K. D., "Circular polarization in atmospheric aerosols," *Atmos. Chem. Phys.* **22**(20), 13581–13605 (2022).

[4] Jacques, S. L., Roman, J. R., and Lee, K., "Imaging superficial tissues with polarized light," *Lasers Surg. Med.* **26**(2), 119–129 (2000).

[5] Hickman, D., Smith, M. I., Kim, K. S., and Choi, H.-J., "The utility of polarimetry within passive military imaging systems," in [*Security + Defence*], (2017).

[6] Vasilescu, B., Nazè, Y., and Loicq, J., "Solution uniqueness and noise impact in a static spectropolarimeter based on birefringent prisms for full Stokes parameter retrieval," *J. Astron. Telesc. Instrum. Syst.* **6**(2), 1 (2020).

[7] Vasilescu, B., Piron, P., and Loicq, J., "Performance analysis of a spectropolarimeter employing a continuous phase variation," *Opt. Express* **31**(13), 21078 (2023).

[8] Pertenais, M., Neiner, C., Bernardi, P., Reess, J.-M., and Petit, P., "Static spectropolarimeter concept adapted to space conditions and wide spectrum constraints," *Appl. Opt.* **54**(24), 7377 (2015).

[9] Boulbry, B., Ramella-Roman, J. C., and Germer, T. A., "Improved method for calibrating a Stokes polarimeter," *Appl. Opt.* **46**(35), 8533 (2007).